A Detailed Study on the Analysis and Design of Geotextile Reinforced Earth Embankments

Amit Kumar
Department of Civil Engineering, NIT Patna, India
amitk.pg18.ce@nitp.ac.in

Avijit Burman
Department of Civil Engineering, NIT Patna, India
avijit@nitp.ac.in (corresponding author)

Shiva Shankar Choudhary
Department of Civil Engineering, NIT Patna, India
shiva@nitp.ac.in

Received: 10 March 2023 | Revised: 31 March 2023 | Accepted: 4 April 2023

 DOI: https://doi.org/10.48084/etasr.5842

ABSTRACT

The design of a steep reinforced slope with an adequate Factor of Safety (FoS) is a classical geotechnical problem. While designing a reinforced soil slope, it is necessary to accurately determine the tensile force to be resisted by the reinforcement to achieve the target FoS value and the length of the geotextile reinforcement to be provided at the top and bottom of the embankment and perform all the required safety checks. This paper presents an MS Excel spreadsheet using Visual Basic Programming that can be used to perform all the analyses required to design geotextile reinforced soil slopes, considering static and seismic loading conditions. This spreadsheet is capable of searching many slip surfaces repeatedly using Bishop's simplified method to determine the maximum tensile force to be resisted by the reinforcement, its top and bottom lengths, and performs deep-seated failure analysis to identify slip surfaces beyond the reinforced zone. This paper reports the results of an illustrative example to highlight all the above-mentioned issues. The results were also compared with the design charts reported in previous studies. The proposed platform can successfully perform all the necessary analyses to design both homogenous and non-homogenous embankments with geotextile reinforcements.

Keywords-geotextile; reinforced slope design; deep-seated failure; Bishop's simplified method; seismic analysis

I. INTRODUCTION

Civil engineers frequently utilize reinforced soil structures to stabilize embankments and slopes. Geosynthetic reinforced soil slope stability has been analyzed in [1]. Various natural and man-made factors may lead to slope instability [2]. Different factors such as soil strength parameters, ambient circumstances, groundwater level, stress history, and natural slopes on hillsides pose different stability concerns for man-made slopes [3]. Cuts and berms differ significantly in man-made elevations. Slope stabilization devices can stabilize unstable slopes [3], while slope stabilization methods reduce driving forces, increase resisting forces, or both. Traditional rehabilitation of embankments and cut slopes sometimes requires removing slide debris and replacing it with free-draining granular materials. An alternative restoration method uses geosynthetics (geotextiles or geogrids) as reinforcement to reduce stabilizing costs [4-5]. In past, the performance of a geotextile-reinforced slope and its causes of failure was assessed using centrifuge testing procedures [6]. Centrifuge analysis examines the effects of reinforcement spacing, tensile strength, soil shear strength, etc. The models failed with well-defined shear surfaces across the slope's toe, which matched the results of limit equilibrium-based reinforced slope design methods. According to [7], maximum reinforcement strain occurs near the mid-height of reinforced slopes on the critical failure surface directly below the slope crest. Digital imaging and centrifuge modeling have also been used to examine geotextile-reinforced slope deformation [8-9].

The stability of geo-synthetic reinforced soil structures is most often assessed using the limit equilibrium approach [10-12]. Some studies assume that the mobilized tension in geosynthetic layers is highly non-uniform, with maximum tension mobilized in the reinforcement layer at the slope's toe [13]. However, others believe that it occurs around the mid-height of the slope [14]. The reinforcement layer distribution and sizing depend on the slope's stability, reinforcement layer

force distribution, and slope depth [15]. Fly ash can be used as structural fill in low-lying areas of expanding residential sites, while roadways and embankments are made from coal-fired power station fly ash [16-18].

A major geotechnical challenge is to design and build a steep embankment providing the desired FoS. The design procedure to achieve the target FoS by providing sufficient reinforcements was documented in [19]. This paper presents a spreadsheet that uses the Visual Basic programming language to achieve this goal. This platform can search numerous failure surfaces repeatedly and analyze them using Bishop's simplified method to report the required top and bottom lengths of reinforcement and the maximum tensile force to be resisted by it. In addition, it can also perform deep-seated failure analysis of an embankment to identify the failure surface with the minimum required FoS outside the reinforced zone. This platform can examine both static and seismic loading conditions and pore water pressure loading to perform the necessary analyses. A fly ash-mixed embankment was studied using the developed spreadsheet-based platform and the simulation results were compared with the design chart results provided in [20].

II. METHOD FOR DESIGNING A GEOTEXTILE-REINFORCED SLOPE

This study aimed to design a geotextile-reinforced slope for a target FoS (FoS_T), using the following steps:

- Checking unreinforced stability of the final slope configuration to determine the zone of soil contributing to failure and likely to be dislodged from the original soil mass. FHWA [19] recommends values for sliding, local squeezing/bearing capacity failure, and deep-seated stability.
- Checking the estimated tensile strength of soil reinforcement to achieve the desired FoS with the design chart data provided [20].
- Determination of the mobilized strength, spacing, and the required length of each geotextile layer.
- Checking of the external stability of the reinforced soil slope considering the individual effects of sliding and seismic loading conditions.

A detailed description of these steps follows.

A. FoS Determination Using Bishop's Method

This study used the limit equilibrium technique based on Bishop's simplified method [21] to estimate the FoS of the slope against failure. According to [22], the FoS (F) based on the limit equilibrium method to satisfy the overall moment equilibrium is defined as:

$$F = \frac{\sum_{i=1,..,n}[(c_i' l_i + (N_i - U_i l_i)\tan\varphi')R_c]}{\sum_{i=1,..,n}[W_i x_i + q\beta_i - N_i f_c + k_h W_i e - A_m]} \quad (1)$$

The expression of base normal (N_i) in Bishop's simplified method for the i^{th} slice is obtained by summing slice forces in the vertical direction as follows:

$$N_i = \frac{W_i + q_i - \frac{(c_i' l_i - \mu_i \tan\varphi')\sin\alpha_i}{F}}{\cos\alpha_i + \frac{\tan\varphi' \sin\alpha_i}{F}} \quad (2)$$

where i is the i^{th} slice inside the failure surface, c' is the effective cohesion, l is the slice base length, h is the height of individual slice, R_c is the radius or the moment arm associated with the i^{th} slice, φ' is the effective angle of internal friction, W is the slice weight, N is the total base normal acting at the base of the individual slice, U is the pore-water pressure, q is an external surcharge load, A_m is the resultant external water force, f_c is the perpendicular offset of the base normal force from the center of rotation, e is the vertical distance from the centroid of each slice to the center of rotation, α is the slice base angle, and k_h is the horizontal pseudo-static acceleration coefficient.

B. Entry-Exit Search Method

As it is necessary to adopt a proper strategy to create the failure surface data, this study used an "Entry-Exit" method to develop them. For a set of points lying on the lower and upper surfaces of the slope, a set of intermediate points can be generated on the bisectors of the connecting chords, and the centers of the failure surface can be found with known locations of three points on the arc of the desired slip circle, as shown in Figure 1. The trial surfaces were generated and subjected to a few conditions: (i) A valid trial surface would be only generated when the center of the slip surface does not extend beyond the vertical and horizontal boundaries through points *A* and *D*, respectively, (ii) the center of the slip circle should lie between the vertical distance *H* from the upper surface dictated by line *CD*, where *H* is the height of the slope, and (iii) the trial surface should not intersect the bottom boundary represented by line *EF*. If any trial surface violates any of these conditions, they are termed "invalid" and are not considered for stability analysis.

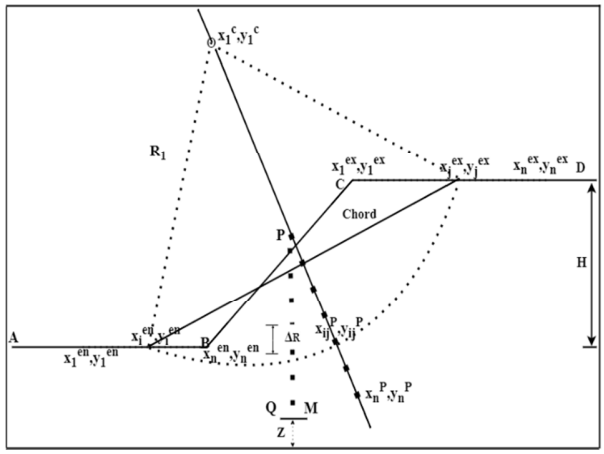

Fig. 1. Entry-exit method.

C. Design of a Stable Reinforced Slope

The developed tensile force in the reinforcement must be determined to determine the stability of the reinforced soil slope. The tensile force generated by the reinforcement contributes to an increased resistance moment around the center of rotation of the circular failure surface. The total

tensile reinforcement per unit width of slope (T_S) to ensure slope stability for each potential failure surface inside the critical zone can be determined from:

$$T_S = (FoS_T - FoS_{UN})\frac{M_D}{D} \quad (3)$$

where FoS_T is the target FoS of the reinforced slope, FoS_{UN} is the FoS of the unreinforced slope, M_D is the disturbing moment trying to cause rotational failure, and D is the moment arm about the center of rotation. Figure 2 shows the general configuration of a geotextile-reinforced slope with embedment length L_e. The minimum FoS, FoS_{min}, the FoS corresponding to a maximum value of T_{max}, and the maximum value of tensile force in geotextile reinforcement can be calculated for the target FoS_T. The horizontal distance from the embankment crest to the point of intersection of the slip surface corresponding to FoS_T provides an estimate of the top reinforcement length L_T.

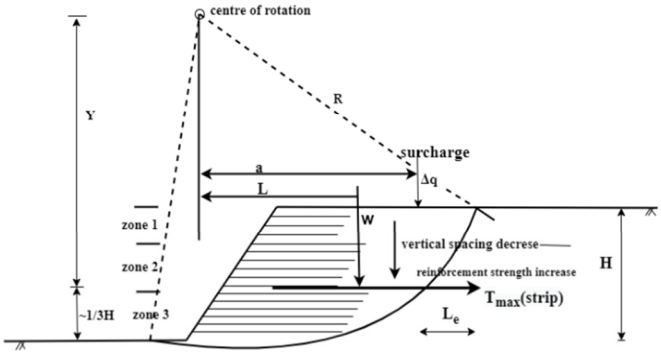

Fig. 2. Rotational shear approach to determine the required strength of reinforcement and reinforcement spacing considerations for high slopes.

D. Checking the Estimated Value with Design Charts

FHWA [19] recommends that the T_S value calculated from (3) should be checked against the design chart values of the tensile forces prescribed by [20]. These charts were developed by performing wedge analysis of geotextile-reinforced slopes made of cohesionless soil. The results were presented in graphical form by combining the results of wedge analysis. The graphs present the values of a few relevant parameters, such as reinforcement force coefficient K and reinforcement length ratios (L_B/H or L_T/H) against different slope angles. The reinforcement force coefficient K determined from these charts can be used to determine $T_{S\text{-}max}$ as follows:

$$T_{S-max} = 0.5K\gamma(H')^2 \quad (4)$$

where $H' = H + \frac{q}{\gamma}$, with q being the surcharge load and γ being the unit weight.

E. Estimation of the Mobilized Strength, Spacing, and the Required Length of Each Geotextile Layer

If the design value of the vertical spacing between N number of geotextile layers is S, then the tensile force experienced by each geotextile layer can be calculated as:

$$T_{S-max} = \frac{T_{zone}\,S}{H_{zone}} = \frac{T_{zone}}{N} \quad (5)$$

TABLE I. TOTAL TENSILE RESISTED BY GEOTEXTILE LAYERS

Zone for distribution of Geotextile	
For 2 zones (H < 6m)	**For 3 zones (H > 6m)**
T_{Bottom}=3/4 $T_{S\text{-}max}$ T_{Top}=1/4 $T_{S\text{-}max}$	T_{Bottom}=1/2 $T_{S\text{-}max}$ T_{Middle}=1/3 $T_{S\text{-}max}$ T_{Top}=1/6 $T_{S\text{-}max}$

F. Check for External Stability

The length of the geotextile reinforcement to be provided at the bottom of the embankment L_B is found by checking the sliding stability of the embankment. In this approach, based on Figure 3, an active wedge was considered at the rear of the reinforced soil mass with the back of the wedge reaching up at an angle of $45^0+\varphi/2$. Equating the driving force produced by active pressure and the resistance obtained from friction at the interface of the embankment, the bottom reinforcement length L_B can be found using the following relationships:

$$Resisting\ Force = FoS \times Sliding\ Force$$

$$(W + P_a sin\varphi_b)tan\varphi_{min} = FoSP_a cos\varphi_b \quad (6)$$

$$W = \frac{1}{2}L^2\gamma_r \tan\theta_r \text{ , for } L < H \quad (7)$$

$$W = [LH - \left(\frac{H^2}{2\tan\theta}\right)]\gamma_r \text{ for } L > H \quad (8)$$

$$P_a = \frac{1}{2}\gamma_b H^2 K_A \quad (9)$$

where L is the length of the bottom reinforcing layer, H is the slope height, FoS is the factor of safety criterion for sliding (>1.3), P_a is the active earth pressure, K_A is the coefficient of active earth pressure, φ_{min} is the minimum angle of shearing friction either between reinforced soil and reinforcement or the friction angle of the foundation soil, θ is the slope angle, γ_r and γ_b are the unit weights of the reinforced and retained backfill, respectively, and φ_b is the friction angle of retained fill.

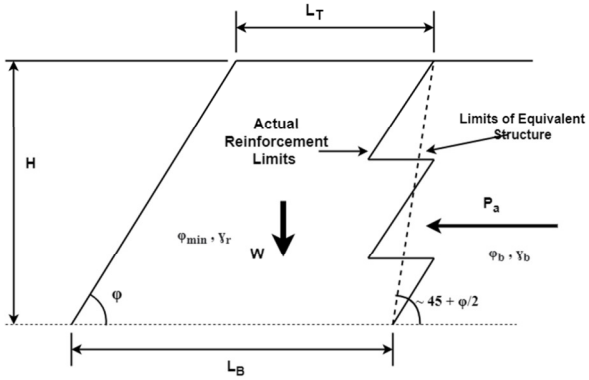

Fig. 3. Sliding stability analysis.

Considering two cases, i.e. $L<H$ or $L>H$, the following expressions can be obtained to calculate L_B:

For $L>H$:

$$\frac{L}{H} = \frac{1}{2\gamma_r \tan\phi_m}\left[\gamma_b K_A \cos\phi_b\,(FOS - \tan\phi_b \tan\phi_m) + \frac{\gamma_r \tan\phi_m}{\tan\theta}\right] \quad (10)$$

For $L<H$:

$$\frac{L}{H} = \sqrt{\frac{K_A \gamma_b (FOS \cos \phi_b - \tan \phi_m \sin \phi_b)}{\gamma_r \tan \theta_r \tan \phi_m}} \quad (11)$$

G. Check for Deep-Seated Global Stability of the Reinforced Embankment

It is further necessary to check that adequate safety for all those slip circles extending beyond the reinforced zone of the embankment is available. FHWA [19] recommends that a minimum of 1.30 should be maintained for all slip surfaces beyond the reinforced zone governed by:

$$FoS_{deep} = \frac{M_R}{M_D} \geq 1.3 \quad (12)$$

where M_D and M_R are the disturbing and resisting moments, respectively.

H. Determination of Embedment Length of Reinforcement and Check against Pull-Out

The embedment length L_e that extends beyond the rotational failure surface of the circular failure surface should be determined from the consideration that adequate pull-out resistance must be available for the provided reinforcement layers. The embedment length L_e can be calculated using:

$$L_e = \frac{T_{S-max}^{layer} FOS_{pull-out}}{F^* \alpha \sigma_v C} \quad (13)$$

where L_e is the embedment or adherence length in the resisting zone behind the failure surface and the minimum value is 1.0m, C is the reinforcement effective unit perimeter, e.g. C = 2 for strips, grids, and sheets, F^* is the pull-out resistance or friction-bearing interaction factor, and α is a scale effect correction factor to account for a non-linear stress reduction over the embedded length of highly extensible reinforcements based on laboratory data. FHWA [19] recommends α parameter values for different reinforcement material choices for extensible reinforcements such as geotextile, and it can be taken as 0.60. Finally, σ_v is the effective vertical stress at the soil-reinforcement interfaces.

I. Seismic Stability of the Embankment

The dynamic stability of the embankment should also be examined by the pseudo-static approach, applying horizontal and vertical earthquake excitations. The recommended minimum value for seismic analysis is:

$$FOS_{seismic} = 1.1 \quad (14)$$

III. RESULTS

A spreadsheet was developed based on the prescribed method for designing geotextile-reinforced slopes and an example case was investigated based on the suggested approach. Reinforced earth slopes consisting of fly ash-based fill materials have many benefits, including low unit weight, resulting in lower net pressure imparted on the foundation soil and reuse of waste material generated from coal-based thermal power plants.

A. Problem 1. Reinforced Slope Design

A 1H:1V geotextile reinforced road embankment made of fly ash mixed soil on the existing ground was required, with an angle of inclination of the slope β=45^0 and height H=5.0m. The design surcharge load was q=10.0kN/m, and the geotechnical properties of the foundation soil and the embankment fill material are mentioned below:

TABLE II. SOIL PARAMETER DATA

	Φ'	c'	γ
Soil	**[°]**	**[kN/m^2]**	**[kN/m^3]**
1	25	0	18
2	17	26	19

An entry-exit search method was employed to find the critical failure surface with the minimum FoS, the reinforcement length L_T to be provided at the top of the slope, and the failure surface corresponding to the maximum design total tensile force (T_S). Only "Toe failures" were investigated for this problem. The target FoS (FoS_T) value for which the slope was analyzed was FoS_T=1.30.

B. Calculation of the Maximum Reinforcement Tension Required to Obtain the Target FoS

The total tensile force T_S to be resisted by the geotextile reinforcement was calculated by (3). For all choices of the center of slip surfaces, the corresponding values of the disturbing moment M_D and the lever arm D were substituted to obtain the T_S values. $T_{S\text{-}max}$ is the maximum of all these estimated T_S values. In Table III, $T_{S\text{-}max}$ is designated as $FoS_{TS\text{-}max}$. Table III also contains the value estimated by the Slope/W software. It can be noted that the result of the spreadsheet matched very well with that of the Slope/W software. The stability of the seismic slope stability was verified considering a horizontal seismic coefficient value k_h=0.08, and a FoS_T=1.10 was used while performing the seismic slope stability analysis. Moreover, the required length of reinforcement to be provided at the top of the slope L_T can be determined, as shown in Figure 4.

TABLE III. FOS VALUES OF BISHOP'S SIMPLIFIED METHOD

Analysis type	**FoS_{min}**	**Validation (slope/W)**	**$FoS_{TS\text{-}max}$**	**No of valid slip surface**	**Run time (s)**
Static	0.600	0.589	0.783	180266	532.02
Seismic k_h=0.08	0.421	0.413	0.680	180286	550.40

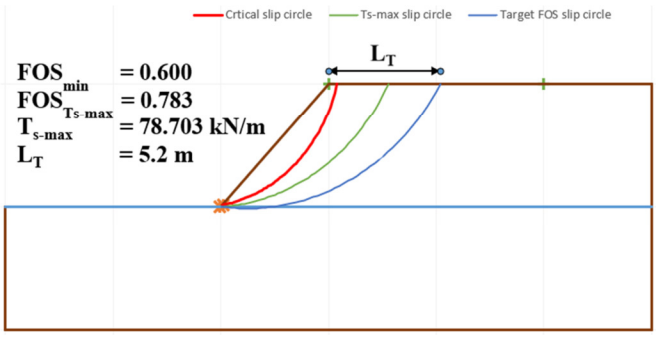

Fig. 4. Static slope analysis results.

Table IV shows the L_T and $T_{S\text{-}max}$ values obtained from the stability analysis using Bishop's simplified method [21]. The values of $T_{S\text{-}max}$ were further compared with the design chart estimation of the maximum tensile force to be resisted by the

geotextile reinforcement based on the results provided in [20]. These design chart-based $T_{S\text{-}max}$ values were calculated using (4) and designated as T_{S-max}^{check}. Table IV also shows the values of K, γ, and H'.

TABLE IV. RESULT AND CHECK OF THE MAX TENSION REINFORCEMENT

Analysis type	L_T (m)	$T_{S\text{-}max}$ (kN/m)	K	γ (kN/m^3)	H' (m)	T_{S-max}^{check} (kN/m)
Static	5.20	78.703	0.25	18.0	5.55	68.062
Seismic	4.80	69.212	NA	NA	NA	NA

Table IV shows that $T_{S\text{-}max}$ agrees reasonably well with the chart value of T_{S-max}^{check} for this problem. However, it should be noted that these analyses were performed in [20] without considering the presence of a water table and only for static loading conditions. If the actual slope conditions vary from those considered in [20], direct comparison of these two values may not be recommended. In [24], it was stated that a 25% variation between the chart and the computational results is acceptable from all practical points of view. A lower target FoS_T was used during seismic slope analysis because it would be uneconomical to use FoS_T=1.30, as seismic excitation occurs only for a brief time. As $FoS_{TS\text{-}max}$ and $T_{S\text{-}max}$ are higher in the case of static analysis, the design of the reinforced slope should be governed only by the results obtained from static analysis.

C. Calculation of Bottom Reinforcement Length LB and Reinforcement Design

It is further necessary to determine the bottom reinforcement length L_B to be provided at the bottom of the embankment. The L_B length was calculated using wedge sliding analysis following (10)-(11). Table V shows the estimated bottom reinforcement length L_B for the current slope. For this problem, a reinforcement spacing S_V=400mm was used to avoid wrapping of the face and surficial stability issues. Therefore, the total number of geotextile layers was obtained by dividing the height of the embankment by the spacing of geotextile layers, i.e. N=5m/0.40m=12.5. Hence, 12 geotextile reinforcement layers can be provided with the bottom layer placed after the first lift of the embankment fill. Table V lists L_B, the spacing of the geotextile layers and their number N, and the T_{S-max}^{layer} for both static and seismic cases.

TABLE V. LENGTH OF THE GEOTEXTILE (TOP AND BOTTOM) LAYERS

Analysis type	L_B (m)	$T_{S\text{-}max}$ (kN/m)	Spacing (S_V) (m)	No. of layers (N)	T_{S-max}^{layer} (kN/m)
Static	6.70	78.703	0.4	12	6.55
Seismic	6.70	69.212	0.4	12	5.76

D. Embedment Length of Reinforcement and Checking Against Pull-Out

The spreadsheet estimated the embedment length of geotextile reinforcement L_e by subtracting the distance from the slope crest to the point of intersection of the failure surface corresponding to $T_{S\text{-}max}$ from L_T. The distance from the slope crest to the point of intersection of the failure surface corresponding to $T_{S\text{-}max}$ is denoted as $L_{TS\text{-}max}$. The spreadsheet calculated the $L_{TS\text{-}max}$ and $L_{TS\text{-}max}$ values at a different depth z from the top surface of the embankment. Table VI summarizes the values of L_T, $L_{TS\text{-}max}$, L_e, vertical overburden pressure σ_v, and $FoS_{pull\text{-}out}$. The value of $FoS_{pull\text{-}out}$ was calculated with (13), where C=2, F^*=0.67, tanφ'=0.204, α=0.60, and the unit weight of embankment fill γ_b^f=18.0kN/m^3. It is further observed that $FoS_{pull\text{-}out}$ was lowest near the top of the slope and increased gradually with depth z. It can be seen that $FoS_{pull\text{-}out}$>1.50 at all depths, which is the minimum recommended by [19]. Thus, the adequacy of the provided L_T at different depths can be checked.

TABLE VI. CALCULATION AND CHECK FOR $FOS_{PULL\text{-}OUT}$ DURING STATIC SLOPE ANALYSIS

z (m)	L_T (m)	$L_{T_{S-Max}}$ (m)	L_e (m)	σ_v	T_{S-max}^{layer} (kN/m)	$FOS_{pull\text{-}out}$
0.3	20.20	17.10	3.10	13.6	6.55	3.00
0.6	20.12	17.10	3.02	20.8	6.55	3.95
1.0	20.00	17.09	2.91	28.0	6.55	5.13
1.4	19.79	17.08	2.71	35.2	6.55	6.00
1.8	19.59	17.07	2.52	42.4	6.55	6.72
2.2	19.39	17.02	2.37	49.6	6.55	7.40
2.6	19.18	17.00	2.18	56.8	6.55	7.79

In the case of seismic loading, the obtained values were compared to the minimum suggested value of 1.50 to determine whether the projected embedded length is enough for the current situation, as shown in Table VII. The estimated L_e was lower than the obtained from static analysis because FoS_T was lower. It is also worth noting that $FoS_{pull\text{-}out}$ was lowest towards the top of the slope and progressively increased with depth z.

TABLE VII. CALCULATION AND CHECK FOR $FOS_{PULL\text{-}OUT}$ DURING SEISMIC SLOPE ANALYSIS

z (m)	L_T (m)	$L_{T_{S-Max}}$ (m)	L_e (m)	σ_v	T_{S-max}^{layer} (kN/m)	$FOS_{pull\text{-}out}$
0.3	19.60	17.64	1.96	15.4	5.76	2.16
0.6	19.41	17.41	2.00	20.8	5.76	2.97
1.0	19.21	17.18	2.04	28.0	5.76	4.08
1.4	18.82	16.87	1.96	35.2	5.76	4.93
1.8	18.43	16.56	1.88	42.4	5.76	5.69
2.2	18.24	16.24	1.99	49.6	5.76	7.07
2.6	17.65	15.62	2.03	56.8	5.76	8.24

E. Checking of the Reinforcement Length

It is necessary to check the simulated values of L_T and L_B with the design chart values [20]. The simulated L_B results are provided in Tables VI and VII, respectively. Corresponding to a value of φ_f'=25^0, the study in [20] provides L_T/H'=0.9, and therefore, L_T^{exp}=4.95m. It can be observed that the computed simulated values satisfied L_T>L_T^{exp}, therefore, they were more conservative estimates. Therefore, L_T=5.20m was adopted as the final design value of the top reinforcement length. However, the tests in [20] were only performed on dry cohesionless sand and the effect of water pressure was not investigated. Similarly, the method in [20] provides an estimate of L_B/H'= 1.4, and hence, L_B^{exp}=7.80m. Although the problem considered does not exactly match the test conditions, it would be safer to consider the higher value of the bottom reinforcement against sliding failure; therefore, L_B=7.80m is recommended.

F. Check for Deep-Seated Global Stability

All failure surfaces extending beyond the reinforced zone were investigated and the slip surface corresponding to the minimum FoS was identified. For all slip surfaces beyond the reinforced zone, a FoS_{deep} of 1.99 was obtained. Similarly, during seismic analysis, a FoS_{deep} of 1.71 was obtained. As per (12), a minimum FoS value of 1.30 must be maintained for the deep-seated failure condition. Therefore, the provided reinforcement length was considered to be adequate. If any slip surface with FoS<1.30 had been located, it would require extending the bottom reinforcements beyond the deep-seated slip surface with the corresponding value of FoS_{min}. The spreadsheet automatically reported all associated data of the slip circle with FoS_{min}. Table VIII and Figure 5 show the results of the deep-seated stability analysis.

TABLE VIII. CALCULATION OF DEEP-SEATED FAILURE SURFACES

Type	L_T (m)	L_B (m)	*FOS*	Valid slip surface	Run time (s)
Static	5.2	7.8	1.99	3407	8.38
Seismic	4.8	NA	1.71	3407	8.32

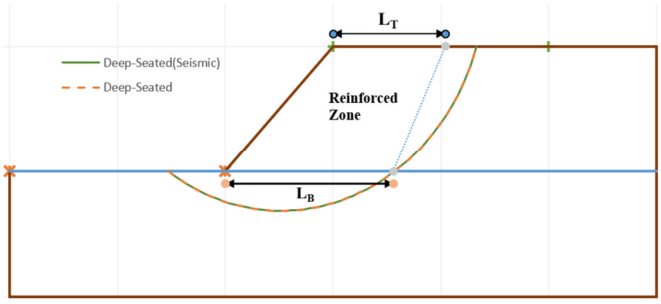

Fig. 5. Deep-seated slope stability check.

G. Design Summary

The final design summary results of the geotextile-reinforced slope include the following specifications:

- Numbers of geotextile layers: For this problem, N=12 geotextile layers are sufficient.
- Length of the geotextile layer to be provided at the top surface L_T: For this problem, L_T=5.20m is recommended.
- Length of the geotextile layer to be provided at the bottom of the embankment: L_B=7.80m.

Figure 6 shows the slope diagram with all the necessary details.

IV. DISCUSSION

A versatile MS Excel spreadsheet using the Visual Basic programming language was developed to analyze a geotextile-reinforced earth embankment and meet the target FoS value. In the future, the platform can be used to develop design charts for determining top and bottom reinforcement length ratios (i.e. L_T/H and L_B/H), considering pore water pressure loading. This platform can also perform deep-seated failure analysis. As commercial software, such as Slope/W, does not perform such analyses, the development of such a platform should be regarded as a welcome addition to the geotechnical software pool.

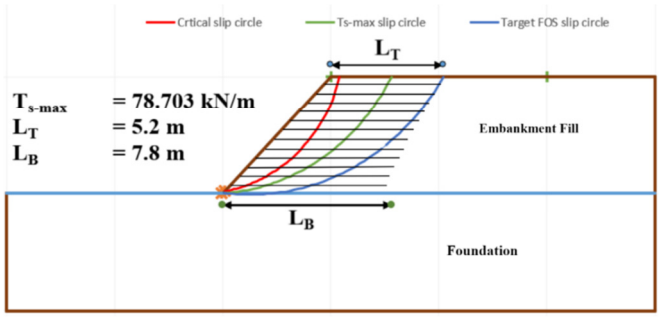

Fig. 6. Details of the geotextile-reinforced slope.

V. CONCLUSIONS

This paper described the development of an MS Excel spreadsheet for designing geotextile-reinforced slopes using Visual Basic programming. The limit equilibrium method based on Bishop's simplified method [21] was used to carry out the slope analysis. The spreadsheet performs slope analysis for a target FoS value under both static and seismic loading conditions and also determines the maximum tensile force that reinforcement must resist to achieve it, along with the length of reinforcement to be provided at the top and bottom of the embankment. This spreadsheet can successfully search for numerous failure surfaces to achieve its objectives and reliably report the desired results. This spreadsheet can be used to perform deep-seated stability analysis to identify the failure surface with minimum FoS extending beyond the reinforced zone. An illustrative example was presented in detail, showing that static analysis governs the determination of the maximum tensile force to be resisted by geotextile layers because the seismic analysis is usually performed with a lower target FoS.

REFERENCES

[1] J. N. Mandal and L. Labhane, "A procedure for the design and analysis of geosynthetic reinforced soil slopes," *Geotechnical & Geological Engineering*, vol. 10, no. 4, pp. 291–319, Dec. 1992, https://doi.org/10.1007/BF00880706.

[2] S. K. Shukla, "A study on causes of landslides in Arunachal Pradesh," in *Proceedings of the Indian Geotechnical Conference*, 1997, pp. 613–616.

[3] M. Shinoda and Y. Miyata, "PSO-based stability analysis of unreinforced and reinforced soil slopes using non-circular slip surface," *Acta Geotechnica*, vol. 14, no. 3, pp. 907–919, Jun. 2019, https://doi.org/10.1007/s11440-018-0678-x.

[4] H. Venkateswarlu and A. Hegde, "Isolation Prospects of Geosynthetics Reinforced Soil Beds Subjected to Vibration Loading: Experimental and Analytical Studies," *Geotechnical and Geological Engineering*, vol. 38, no. 6, pp. 6447–6465, Dec. 2020, https://doi.org/10.1007/s10706-020-01447-7.

[5] R. Helis, T. Mansouri, and K. Abbeche, "Behavior of a Circular Footing resting on Sand Reinforced with Geogrid and Grid Anchors," *Engineering, Technology & Applied Science Research*, vol. 13, no. 1, pp. 10165–10169, Feb. 2023, https://doi.org/10.48084/etasr.5607.

[6] J. G. Zornberg, N. Sitar, and J. K. Mitchell, "Performance of Geosynthetic Reinforced Slopes at Failure," *Journal of Geotechnical and Geoenvironmental Engineering*, vol. 124, no. 8, pp. 670–683, Aug. 1998, https://doi.org/10.1061/(ASCE)1090-0241(1998)124:8(670).

[7] J. G. Zornberg and F. Arriaga, "Strain Distribution within Geosynthetic-Reinforced Slopes," *Journal of Geotechnical and Geoenvironmental*

Engineering, vol. 129, no. 1, pp. 32–45, Jan. 2003, https://doi.org/10.1061/(ASCE)1090-0241(2003)129:1(32).

[8] B. V. S. Viswanadham and R. R. Mahajan, "Centrifuge model tests on geotextile-reinforced slopes," *Geosynthetics International*, vol. 14, no. 6, pp. 365–379, Dec. 2007, https://doi.org/10.1680/gein.2007.14.6.365.

[9] H. E. Fazazi, M. Elgarej, M. Qbadou, and K. Mansouri, "Design of an Adaptive e-Learning System based on Multi-Agent Approach and Reinforcement Learning," *Engineering, Technology & Applied Science Research*, vol. 11, no. 1, pp. 6637–6644, Feb. 2021, https://doi.org/10.48084/etasr.3905.

[10] U. R. Albino, F. H. M. Portelinha, and M. M. Futai, "Numerical simulation of a geotextile soil wall considering soil-atmosphere interaction," *Geosynthetics International*, vol. 27, no. 4, pp. 394–413, Aug. 2020, https://doi.org/10.1680/jgein.20.00003.

[11] G. B. Nunes, F. H. M. Portelinha, M. M. Futai, and C. Yoo, "Numerical study of the impact of climate conditions on stability of geocomposite and geogrid reinforced soil walls," *Geotextiles and Geomembranes*, vol. 50, no. 4, pp. 807–824, Aug. 2022, https://doi.org/10.1016/j.geotexmem.2022.04.004.

[12] R. M. Koerner and G. R. Koerner, "An extended data base and recommendations regarding 320 failed geosynthetic reinforced mechanically stabilized earth (MSE) walls," *Geotextiles and Geomembranes*, vol. 46, no. 6, pp. 904–912, Dec. 2018, https://doi.org/10.1016/j.geotexmem.2018.07.013.

[13] F. Vahedifard, K. Mortezaei, B. A. Leshchinsky, D. Leshchinsky, and N. Lu, "Role of suction stress on service state behavior of geosynthetic-reinforced soil structures," *Transportation Geotechnics*, vol. 8, pp. 45–56, Sep. 2016, https://doi.org/10.1016/j.trgeo.2016.02.002.

[14] X. L. Yang and J. H. Chen, "Factor of Safety of Geosynthetic-Reinforced Slope in Unsaturated Soils," *International Journal of Geomechanics*, vol. 19, no. 6, Jun. 2019, Art. no. 04019041, https://doi.org/10.1061/(ASCE)GM.1943-5622.0001399.

[15] H. Djeffal and S. Belkacemi, "A New Approach for Evaluating the Soil Slope Reinforcement Tensile Forces Using Limit Equilibrium Methods," *Geotechnical and Geological Engineering*, vol. 39, no. 3, pp. 2313–2327, Mar. 2021, https://doi.org/10.1007/s10706-020-01628-4.

[16] R. K. Arvind, P. Biswajit, and S. Gurdeep, "A Study on Backfill Properties and Use of Fly Ash for Highway Embankments," *Journal of Advanced Laboratory Research in Biology*, vol. 1, no. 2, 2022.

[17] M. Touahmia, "Performance of Geosynthetic-Reinforced Soils Under Static and Cyclic Loading," *Engineering, Technology & Applied Science Research*, vol. 7, no. 2, pp. 1523–1527, Apr. 2017, https://doi.org/10.48084/etasr.1035.

[18] M. Touahmia, H. Gasmi, and M. A. Said, "Creep Performance of Geosynthetic Reinforcements," *Engineering, Technology & Applied Science Research*, vol. 10, no. 4, pp. 6147–6151, Aug. 2020, https://doi.org/10.48084/etasr.3717.

[19] V. Elias, B. R. Christopher, R. R. Berg, and Inc. Ryan R. Berg & Associates, "Mechanically Stabilized Earth Walls and Reinforced Soil Slopes: Design and Construction Guidelines (Updated Version)," FHWA-NHI-00-043, Mar. 2001.

[20] G. R. Schmertmann, "Design charts for geogrid-reinforced soil slopes," *Geosynthetics*, pp. 108–120, 1987.

[21] A. W. Bishop, "The use of the Slip Circle in the Stability Analysis of Slopes," *Géotechnique*, vol. 5, no. 1, pp. 7–17, Mar. 1955, https://doi.org/10.1680/geot.1955.5.1.7.

[22] D. G. Fredlund and J. Krahn, "Comparison of slope stability methods of analysis," *Canadian Geotechnical Journal*, vol. 14, no. 3, pp. 429–439, Aug. 1977, https://doi.org/10.1139/t77-045.